SERBIAN JOURNAL OF ELECTRICAL ENGINEERING
Vol. 21, No. 2, June 2024, 201-216

UDC: 621.396.674:621.3.011.2 DOI: https://doi.org/10.2298/SJEE2402201M

A Compact High Gain UWB Planar Monopole Antenna Using Circular Slots

Prasan Kumar Mishra[1], Tapan Kumar Patnaik[1], Bhavani Prasad Panda[2], Rabindra Kumar Mishra[1]

Abstract: In this manuscript, the design of a compact-size circular patch Ultra-Wideband (UWB) antenna with enhanced fractional bandwidth (BW), peak realized gain (PRG), and proper impedance matching is presented. The modified antenna has three circular slots etched from the circular path (top), fed by a 50Ω microstrip feed line. These circular slots play a significant role in improving the impedance bandwidth. Additionally, the partial ground plane with a slot integrated with a rectangular stub is used in order to achieve a bandwidth for an operating range of 3.25 GHz – 27 GHz. The proposed antenna is designed, fabricated, and tested in the laboratory in order to validate with simulation data. The designed antenna size is 25 mm × 20 mm × 0.508 mm. The experimental value of 10 dB return loss absolute/fractional BW of 23.75 GHz/157.08% at the center frequency, minimum/ maximum gain of 5.90/12.05 dBi, and maximum /minimum radiation efficiency of 85/97 % are achieved from the 3.25 GHz to 27 GHz frequency range. In addition, a comparison table is provided to prove the state-of-the-art of the antenna's design. The proposed antenna is suitable for wireless services, radar, and satellite communication.

Keywords: Circular slot, Impedance bandwidth, Improved gain, Ultra-wideband.

1 Introduction

Nowadays, an ultra-wideband (UWB) antenna is required for better communication as It provides better data rates and has different applications in a particular frequency band. However, the Federal Communication Commission (FCC) fixed the UWB range's bandwidth (3.1 GHz – 10.6 GHz) in February 2002 [1]. The rapid increase in demand for communication in wideband significantly requires a high data rate. In order to fix the UWB range, the FCC has set the unlicensed frequency band from 3.1 GHz to 10.6 GHz as UWB. A UWB antenna covers an impedance bandwidth of 500 MHz or more for commercial utilization with a power limit of –41.3 dBm/MHz, as assigned by FCC [1].

[1]GIET University, Deparment of Physics, Gunupur, Odisha, India;
E-mails: pkmishra@giet.edu, tapanpatnaik@giet.edu, rabindramishra@giet.edu
[2]Deparment of Physics, Chikiti Mahavidyalaya, Chikiti, Odisha, India; E-mail: nulu22@yahoo.com

UWB antenna characteristics like high-speed transmission, compact size, simplicity of incorporation with other devices, stable radiation pattern, high gain and radiation efficiency, and proper impedance matching make them alluring for indoor and outdoor hand-held applications [2]. Over the last few decades, tremendous work on UWB antennas has been reported in [3–6] with different shapes and techniques to improve impedance bandwidth. Bandwidth enhancement using slots and the modified ground has been presented in [3] with the dimensions of 25 mm × 30 mm × 1.6 mm. The authors in [4] presented a technique for improved bandwidth by optimizing the gap between rectangular and ground planes. For that the authors considered the antenna size of 50 mm × 90 mm × 1.52 mm. In [5], the authors have designed a hexagonal-shaped antenna of dimensions 34 mm × 28 mm × 1.6 mm for WLAN application. Recently, a metamaterial integrated antenna has been proposed in [6] for bandwidth enhancement with a geometry of 42 mm × 50 mm × 2.1 mm. It used SSR in place of Rogers RO4003. Many designs on UWB antennas have recently been reported in [7–14]. In order to achieve enhanced bandwidth and improve the other antenna characteristics, the electromagnetic bandgap (EBG) [10], symmetrical hexagonal structure [11], Z-shaped with stepped meandering line [12], and a Ribbon-shaped slot [13] have been implemented in the antenna structure. A few new modeling UWB antennas for specific applications [14–17] have been developed recently. In [14], a UWB planar monopole array has been designed to reduce the radar cross-section. A shielded planar array of active slot antennas has been suggested in [15] for breast microwave imaging applications. A revolutionary automatic vehicle recognition system based on a UWB antenna for radar has been reported in [16]. Moreover, low-profile and multiple UWB antennas have been proposed in [17] to combine networks for wireless power transfer applications. Furthermore, to improve the impedance and other radiation characteristics with a specified application, a stack patch antenna [18], a 6×2 linear feed antenna [19], a filter antenna [20], and reflector-based dipole antennas [21] have been discussed.

This paper presents a compact circular monopole antenna with a partial ground plane that archives improved impedance bandwidth and peak realized gain with the modified partial ground plane. A partial ground plane is modified by cutting a rectangular slot from the ground plane, improving impedance matching along with return loss. Moreover, three slots are placed in the radiating part to enhance the impedance bandwidth along with the antenna characteristics like gain and efficiency.

2 Design Antenna

Initially, the proposed antenna geometry uses an FR4 (tm) substrate (20mm × 25 mm×1.6 mm) having a relative permittivity (ε_r) of 4.4 and loss tangent ($\tan \delta$) of 0.02. The 3D, top, and bottom views of the partial and modified ground planes are shown in Figs. 1 and 2. The top side of the monopole antenna consists of a circular radiating patch with three circular slots. A microstrip feed line of the width W_p = 2.5 mm and L_p = 6.35 mm is used in order to achieve a 50Ω matching impedance. In contrast, the bottom side has a slot cut with partial ground integrated with a small rectangular shape of a dimension of $L_3 \times W_3$ (2.6 mm×2 mm). The proposed antenna's radius of the circular radiating patch was calculated manually by the formula [9]. The radius of the circular patch R_1 = 9.1 mm corresponds to the first resonant frequency. From this work, we observed that cutting three annular slots from the radiating patch shifted the first resonant frequency to the lower frequency. The parametric analysis is implemented to fix the L_4 and the radius of circular slots R_z, and R_y. The variation of L_4 from 3.37 to 4.17 mm with a step size of 0.2 mm is analyzed as shown in Fig. 3a. From observations, it is noticed that the L_4 varies with little effect on the return loss. However, the frequency is shifted slightly to down and up. Similarly, the radii of three circular slots are also varied, as shown in Figs. 3b and c. These three circular slots play a significant role in achieving a wider bandwidth. The impedance bandwidth is improved when the R_z and R_y are varied from 2.75 to 4.75 mm and 2.8 to 3.2 mm with step sizes of 0.5 mm and 0.1 mm, respectively. As a result, the values of L_4 = 3.77 mm, R_z = 3 mm, and R_y = 3.75 mm are fixed in proposed antenna. Besides, the width of the substrate and ground plane significantly influences the starting frequency of the monopole antenna. Moreover, decreasing the ground plane's dimensions results in a shorter current path length, which causes poor matching at a lower frequency. To make the compact size and cover a wide bandwidth, the partial ground width, W_T and length, L_5 are fixed at 20 mm, and 6.27 mm, respectively.

In order to improve impedance matching, a rectangular slot is cut from the partial ground plane of size $L_3 \times W_3$ (2.6 mm×2 mm). from the upper side of the ground. Finally, the optimized dimensions of the proposed work are follows: W_p = 2.5 mm, L_p = 6.35 mm, L_1 = 5.25 mm, L_2 = 7.0 mm, W_1 = 1.36 mm, L_3 = 2.6 mm, L_4 = 3.77 mm, L_5 = 6.27 mm, L_6 = 18.73 mm, W_T = 20 mm, L_T = 25 mm, R_1 = 2.5 mm, R_y = 3.75 mm, R_z = 3 mm, h = 1.6 mm for FR4 (h = 0.508 mm for 5880). As we know, the FR4 substrate has a high loss (ε_r = 4.4), so the design cannot measure higher frequency. In this regard, the proposed antenna is simulated and tested with a Rogers RT/Duroid 5880 (tm) substrate (20×25× 0.508) mm^3 having a relative permittivity (ε_r) of 2.2 and loss tangent of 0.0009. The dimensions are the same as those used in the FR4 substrate.

Furthermore, an explanation of the different stages of antenna design further enhances the gain and improves the antenna radiation characteristics, as shown in Fig. 4a. As observed from Fig. 4b (reflection coefficient vs. frequency), the impedance mismatch is found between 8.5 and 11.5 GHz and above 15 GHz in stage 1 (only using the circular patch). At stage 2, a U-shaped slot was etched at the center (the metallic part) from the ground part, keeping the radiating patch in a circular shape.

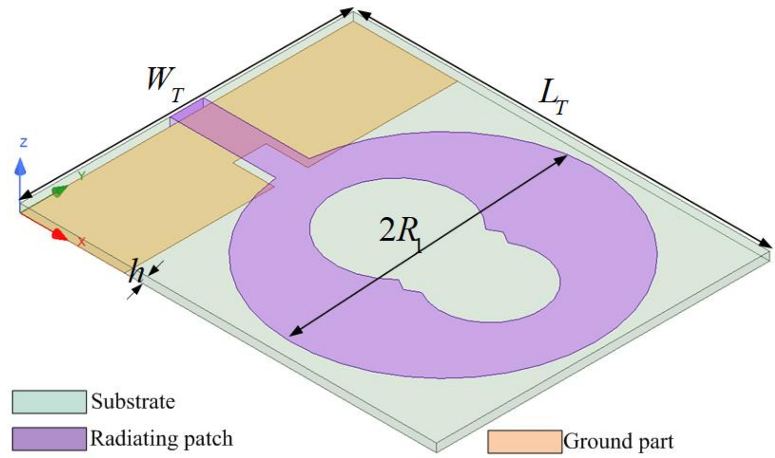

Fig. 1 – *3D view of UWB antenna with partial ground plane.*

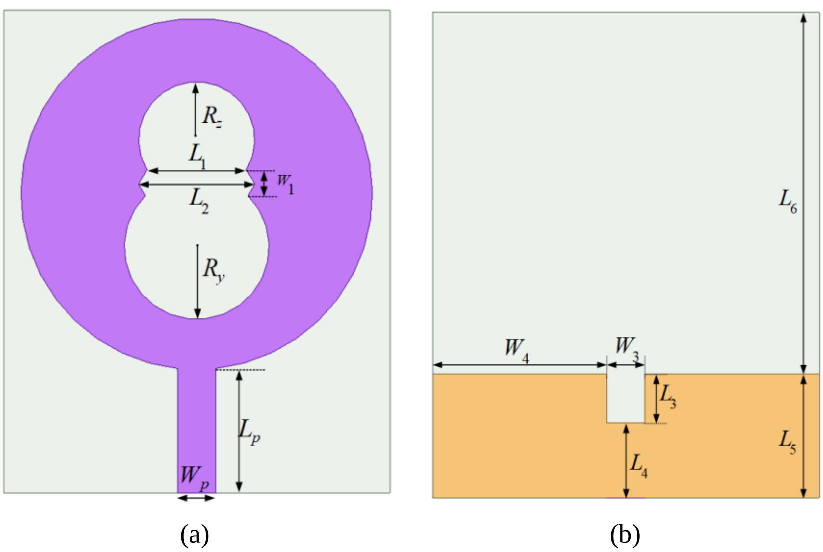

Fig. 2 – *Geometric of proposed antenna:* (a) *front view, and* (b) *bottom view.*

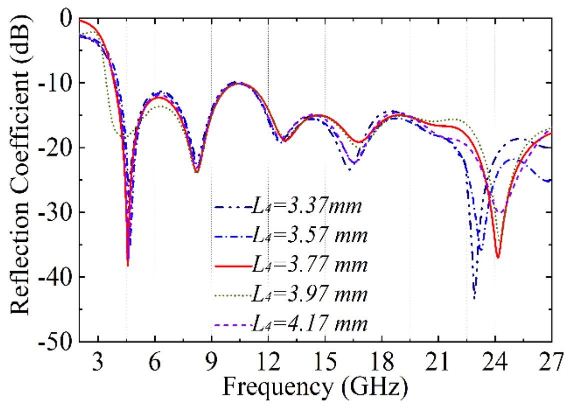

(a)

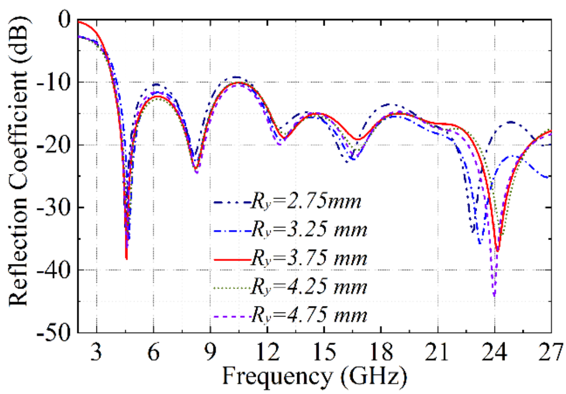

(b)

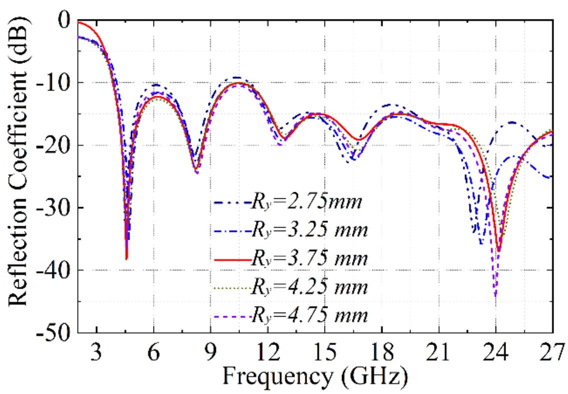

(c)

Fig. 3 – *Reflection coefficient effect on different parameters of the proposed antenna:* (a) L_4, *with* R_y=3.75 mm *and* R_z=3 mm*;* (b) R_y *with* L_4=3.77 mm *and* R_z=3 mm*; and* (c) R_z *with* R_y=3.75 mm *and* L_4=3.77 mm.

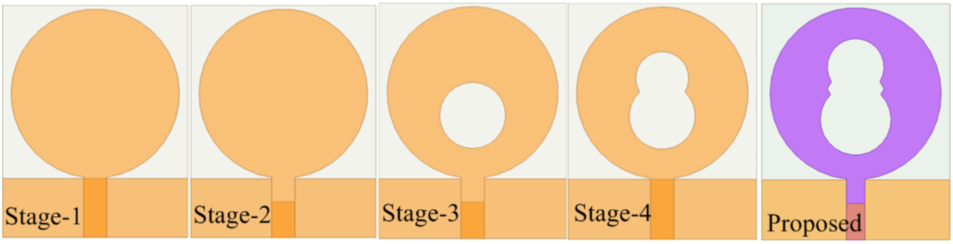

(a)

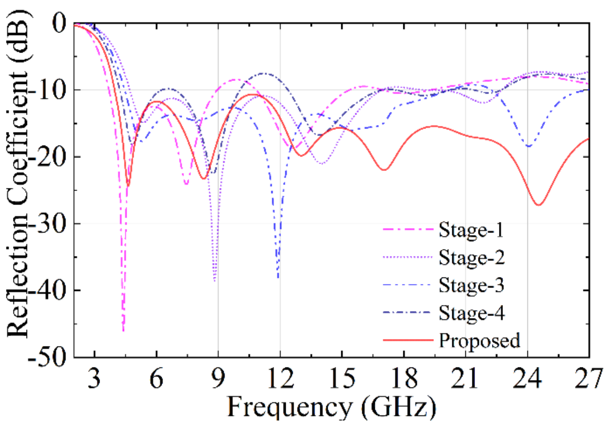

(b)

Fig. 4 – (a) *Different stages of the proposed antenna, and* (b) *Simulated Reflection coefficient at the different stages of the proposed antenna.*

Consequently, the return loss is improved. When a circular slot is etched from the radiating patch (top) at stage 3, which results, the return loss is significantly improving at the higher frequency, i.e., above 15 GHz, as shown in Fig. 4a. At stage 4, another semicircular slot is etched from the radiating patch in addition to a circular slot. The impedance match is disturbed. Finally, the combination of three circular slots is etched from the radiating patch (stages 1–4) and a small circular slot in the proposed design. The return loss is also improved. Hence, all the radiation characteristics and impedance bandwidth also improved. All the dimensions of circular slots are fixed by using parametric analysis.

The surface current distribution is calculated in two different substrates, FR4, and Rogers 5880LZ, with five different resonant frequencies over the band, as depicted in Fig. 5. However, these three frequencies help in plotting the radiation pattern paragraphs clearly as indicated.

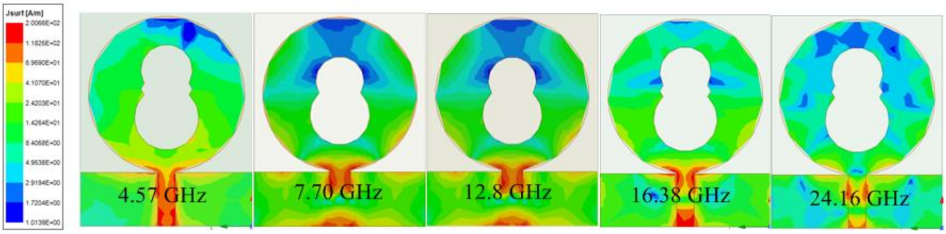

(a)

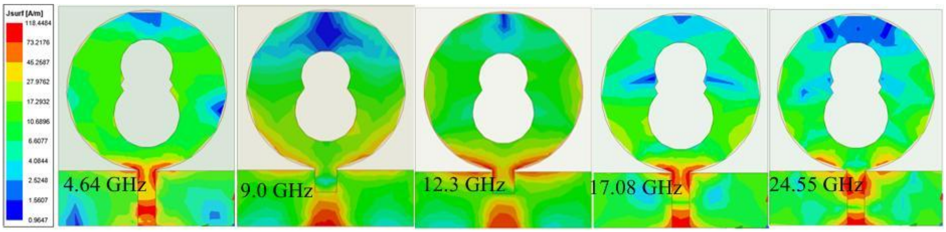

(b)

Fig. 5 – *Surface current distribution top and bottom views at* (a) *FR4, and* (b) *Rogers 5880LZ substrates at different frequencies.*

3 Simulation and Experimental Results

The proposed antenna configuration was designed and simulated using HFSS software. The simulated result achieved bandwidth from 3.25 GHz to 27 GHz for a reflection coefficient less than –10 dB (VSWR < 2). The fabrication porotypes of top and bottom views of two different substrates are shown in Fig. 6. In addition, the antenna and vector network analyzer (VNA) measurement setup to measure the return loss, as shown in Fig. 6.

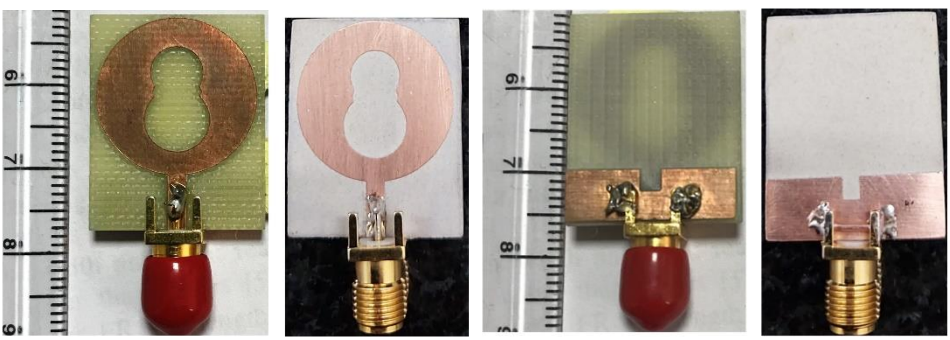

(a) (b)

Fig. 6 – *Laboratory prototype of the proposed antenna (FR4 (left) and 5880 (right)):* (a)*Top and* (b) *Bottom views.*

Fig. 7a shows the measurement setup with FR4 substrate, whereas the Rogers 5880LZ substrate is shown in Fig. 7b. The simulated and measured results of return loss (RL) of both substrates are depicted in Fig. 8 (for (a) FR4, and (b) 5880LZ). It provides measured fractional impedance bandwidth of 157.08 % (simulated: 23.76 GHz and 157.1) at 15.1 GHz (mid or center frequency) and impedance matching over the band. In Fig. 8a, the measured reflection is a slight discrepancy from the simulated results due to the surface wave generation between the SMA connector and fabricated antenna when soldered them.

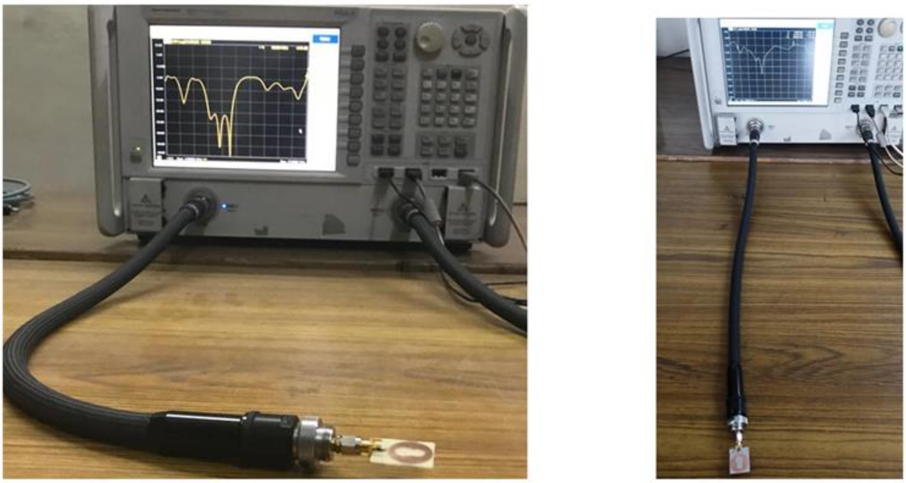

Fig. 7 – *Measurement setup of the proposed antenna FR4 (left) and 5880 (right).*

The stepwise study of making the proposed antenna is shown in Fig. 4a. The introduction of rectangular slot and stub in-ground distribution of surface current changes (see Fig. 5), allows for better impedance matching by varying the length and width of the rectangular slot cut and integrated stub. In parametric analysis, we also conclude that the modified ground's return loss is better than the partial ground's return loss. The antenna has an input impedance of (50.69 – j0.033) Ω and (50.95 + j0.028) Ω at the resonance frequency of 4.64 and 17.08 GHz, respectively.

The antennas are measured in an anechoic chamber, as shown in Fig. 9. The simulated and measured gain of the antenna over the entire bandwidth is depicted in Fig. 10. It can be observed that the minimum-maximum range of measured peak realized gain of 5.9-8.6 dBi and 5.9-12.05 dBi (simulated: 5.9-8.65 dBi and 5.9-14.1 dBi) are obtained for FR4 and 5880LZ substrates, respectively.

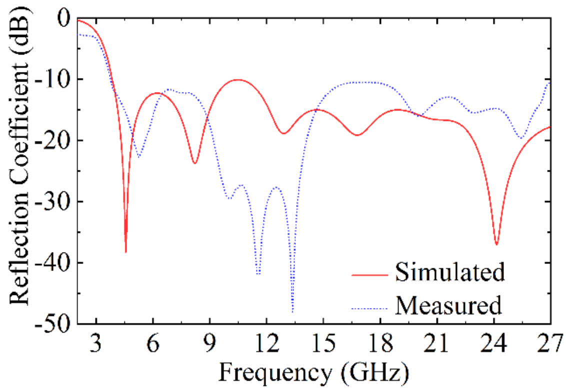

(a)

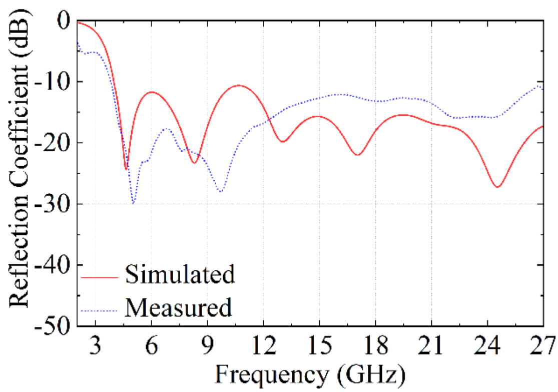

(b)

Fig. 8 – *Simulated and measured reflection coefficient of UWB antenna:* (a) *FR4, and* (b) *Rogers RT/Duroid 5880*.

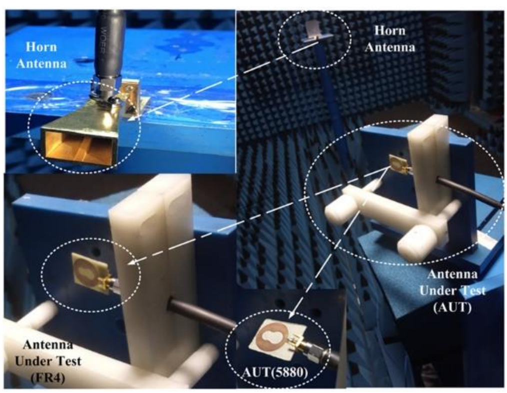

Fig. 9 – *Measurement setup of antenna radiation characteristics (Rogers RT/Duroid 5880 and FR4).*

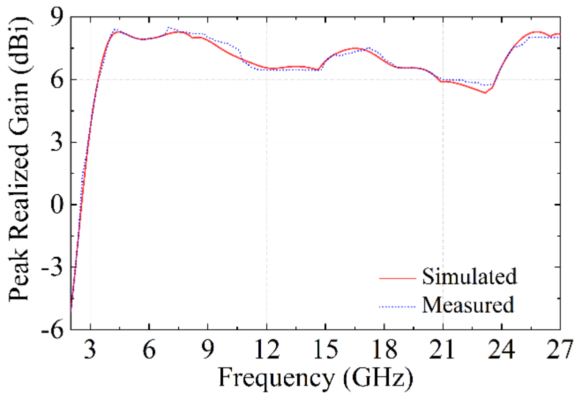

(a)

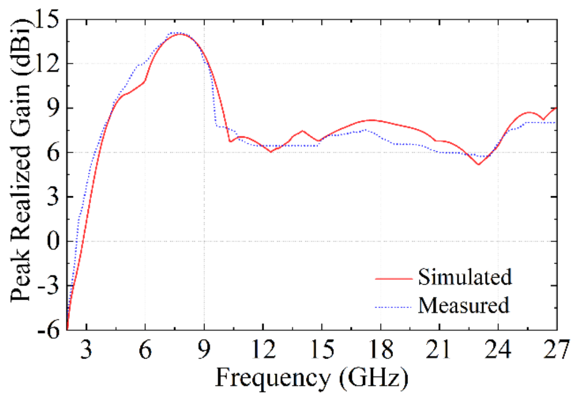

(b)

Fig. 10 – *Simulated and measured peak realized gain of UWB antenna:*
(a) *FR4, and* (b) *Rogers RT/Duroid 5880.*

Also, from Fig. 11, we can see that the proposed design has an average simulated efficiency of more than 81.5 % throughout the frequency band. The simulated minimum and maximum radiation efficiencies are 67 and 96 % for the FR4 substrate. In contrast, the simulated minimum and maximum radiation efficiencies are 85 and 97 % for 5880LZ material. As we can see from the gain and efficiency plots, the gain and efficiency of the proposed antenna fabricated with 5880LZ substrate are better than the FR4 due to loss factor and loss tangent values. Hence, for the reason, the radiation pattern is measured using a 5880LZ substrate.

Moreover, the loss is the main crucial factor of the antenna radiation characteristics. So:

$$Gain = \frac{4\pi U(\theta,\phi)}{P_{rad} + P_{loss}}, \tag{1}$$

where $U(\theta,\phi)$, P_{rad}, and P_{loss} are radiation intensity, radiated power and loss power, respectively.

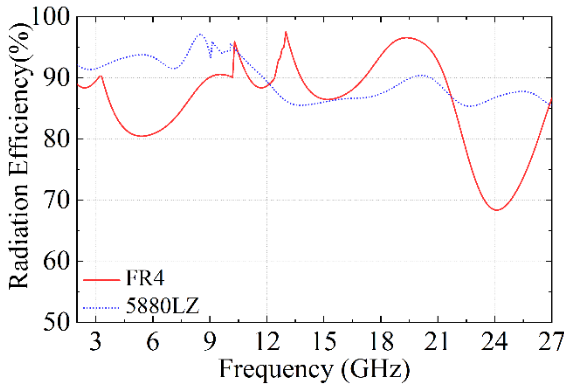

Fig. 11 – *The simulated radiation efficiency of the proposed antenna.*

If the loss is increased, the gain is reduced a little bit. In this case, the gain is enhanced around 1-5 dBi from 4 to 10 GHz frequency range, and constant gain is obtained from 10 to 27 GHz for both cases (For FR4: 5-6 dBi; 5880LZ: 6-8 dBi).

Now, another cause of concern is radiation efficiency. The directivity of both antennas is almost the same. So, the gain is directly proportional to efficiency ($G=\eta D$, D is directivity, and η is the antenna's radiation efficiency). For the FR4 substrate, the radiation efficiency is 67-96 % range, and for the 5880LZ substrate, the radiation efficiency varied from 85 to 97 %. That means the gain increases/ decreases with increases/ decreases of radiation efficiency.

Using the FR4 substrate, the simulated measured normalized radiation patterns are plotted, as shown in Fig. 12. It can be observed that the cross-polarization level is almost nearer to the co-polarization level in both the E- and H-planes of the normalized radiation patterns. Due to the higher loss of the FR4, the cross-polarization level is slightly higher than the Roger substrate. In light of this, the proposed antenna is considered the Roger 5880LZ substrate for antenna fabrication. The antenna simulated and experimental normalized radiation pattern at the resonance frequency of 4.64 GHz, 17.08 GHz, and 24.55 GHz (E- and H-planes), as shown in Fig. 13. It can be observed from the figure that the antenna exhibits an omnidirectional radiation pattern of E-plane, except at 17.08 GHz. Similarly, the proposed antenna is provided with an omnidirectional pattern of H-plane except at 17.08 GHz. It is clearly seen from Figs. 13c and 13d that the E-and H-plane provided a bidirectional pattern. The measured cross-polarization is above 40 dB for both E- and H-plane radiation patterns.

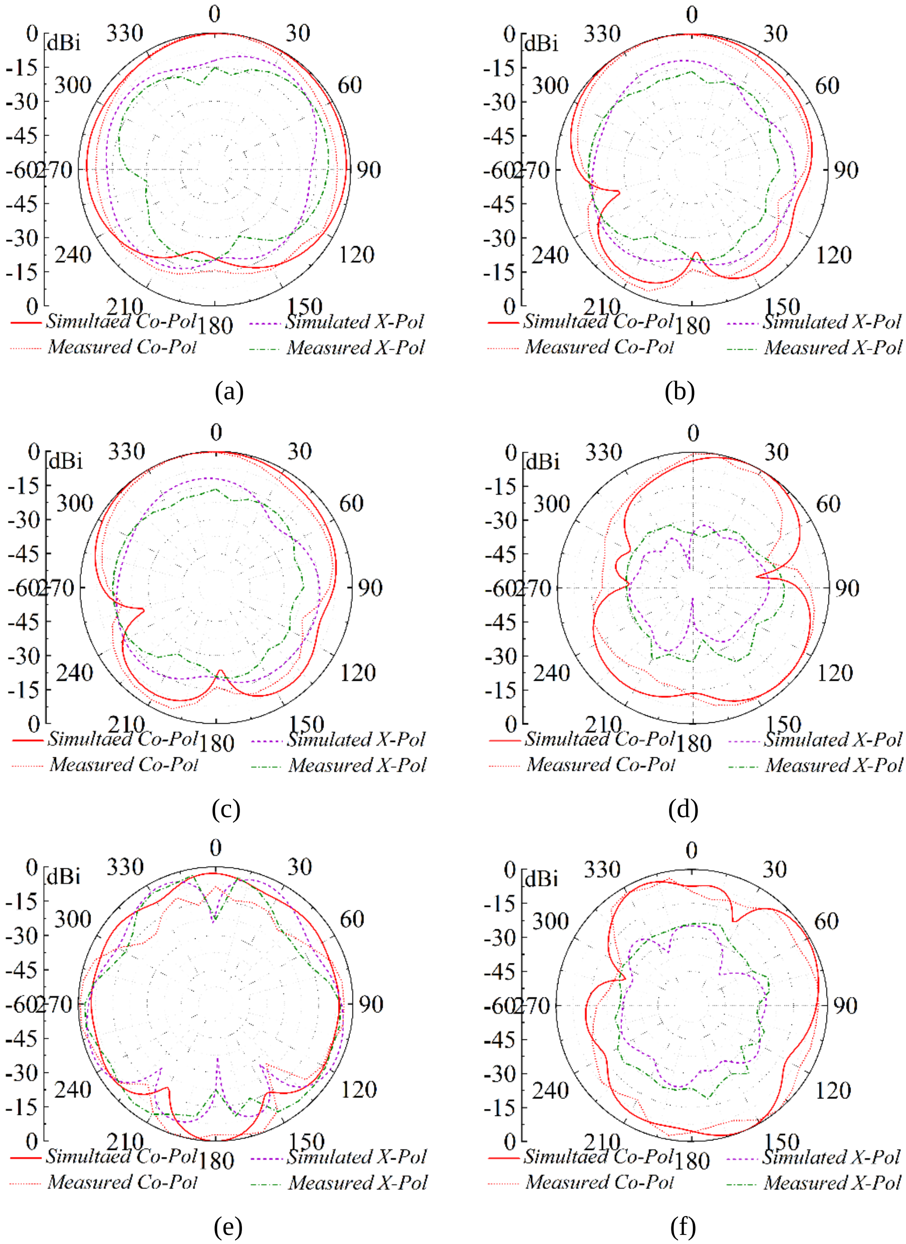

Fig. 12 – *Simulated and measured normalized radiation pattern (FR4):* (a) *E-plane and* (b) *H-plane at* 4.57 GHz*;* (c) *E-plane and* (d) *H-plane at* 12.8 GHz*;* (e) *E-plane, and* (f) *H-plane at* 24.16 GHz.

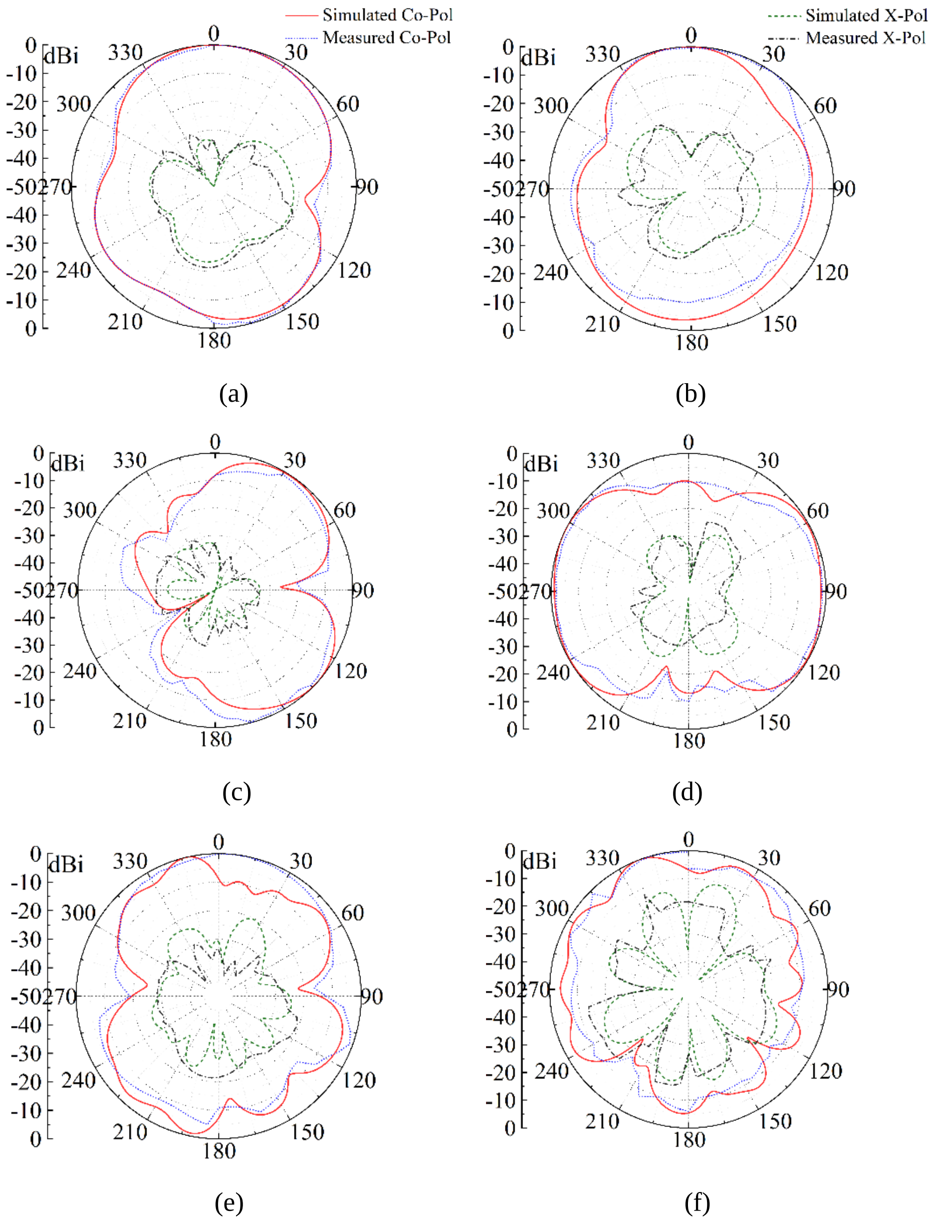

Fig. 13 – *Simulated and measured normalized radiation pattern (5880LZ):* (a) *E-plane and* (b) *H-plane at 4.64 GHz;* (c) *E-plane and* (d) *H-plane at* 17.08 GHz*;* (e) *E-plane and* (f) *H-plane at* 24.55 GHz.

In addition, the figure of merit (FOM) is introduced in this Section in order to add a fair comparison with the proposed work to the state-of-the-art. It is noted that the radiating patch increases with the decrease in resonant frequency. In light of this, the authors restricted the comparison of compact with reported in the lower or higher frequency range. However, the authors have introduced FOM in order to make a fair comparison with the reported previous work. The FOM is defined as:

$$FOM = \frac{B \times G}{V}, \tag{2}$$

where B is the fractional bandwidth calculated at the center frequency, V is normalized volume (volume/λ_0^3), λ_0 is the operating wavelength at a center frequency, and G is the peak realized gain of the antenna (linear scale). Then, the FOM is calculated for each reported work and put in **Table 1**.

Table 1
Comparison of Present Work with the State-of-the-art.

Ref.	Antenna Size (mm^3)	ε_r	Freq. (GHz)	ABW (GHz)	Gain (dBi)	η (%)	FOM	App.
[2]	21.6×12.6×2.4	4.4	2.5-12.5	10	2.6-6.4	80-87.5	37468	S, C, and X Bands
[10]	30.5×31×1.57	2.2	2.64-12.9	10.26	2-6.7	NR	7680	WLAN/X-band
[11]	20×25×1.6	4.4	3.1-12.2	9.1	5.1	NR	29119	Wireless Communic.
[12]	38×35×1.57	2.2	2.8-22.7	19.9	1.6-6.4	70-93	2437.5	Microwave Imaging, Communic.
[13]	20×18×1.6	4.4	3.6-15.5	11.96	4.12	NR	17917	Wireless Communic.
[22]	35×34.8×400	4.4	0-2.5	2.5	3.4-5.46	98	15828	NR
[23]	70×60×0.762	NR	2.5-18	15.5	1.8-5.3	NR	2636	Radar Communic.
[24]	200×125.8×0.60	NR	2-18	16	5-7	NR	1124	NR
This Work	25×20×1.6 25×20×0.508	4.4 2.2	3.27-27 3.25-27	23.73 23.75	5.95-8.6 6-12.05	67-96 85-97	8202 39136	Wireless services, radar, Satellite Communic.

NR: Not reported; ARB: Absolute bandwidth; FOM: Figure of merit; η = efficiency, App: Applications, Communic.: Communications

Finally, a comparison table is made to compare the similar types of UWB planar monopole antenna with the present work mentioned in **Table 1**. The impedance bandwidth (both ABW and FBW), peak realized gain and radiation efficiency are higher than [2, 10 – 13, 22 – 24]. From **Table 1**, the proposed antenna is more compact than [10–12, 22–24] and a little bit higher than [2] and [13]. It is noted that the FOM is higher than the all reported works which are reflected in **Table 1**. The proposed antenna has also tested the low and high-loss substrates to compare with similar state-of-the-art types of designed antenna.

4 Conclusions

A single-layer compact microstrip-fed UWB monopole antenna with a modified ground plane was designed and studied. The modified structure incorporates the partial ground with one rectangular slot integrated with a rectangular stub, which increases the gain and overall performance of the antenna. The substrate FR4 and Rogers RT/Duroid 5880LZ are used and selected due to their low absorption, low electric loss, and flexibility. Suitable impedance matching over the entire band from 3.25 GHz to 27 GHz and 157.28 % bandwidth, a maximum gain of 12.05 dBi, and a maximum efficiency of 97 % over the band (3.25 GHz – 27 GHz). The proposed antenna can be used for various wireless services, radar, and satellite communication applications in C X, Ku, and Ka-bands applications.

5 References

[1] K. Kiminami, A. Hirata, T. Shiozawa: Double-Sided Printed Bow-Tie Antenna for UWB Communications, IEEE Antennas and Wireless Propagation Letters, Vol. 3, 2004, pp. 152 – 153.

[2] A. K. Nayak, D. Gountia, B. K. Turuk, S. B. Panda: Compact UWB Antenna for S, C, and X Bands Applications, Proceedings of the IEEE International Symposium on Smart Electronic Systems (iSES) (Formerly iNiS), Hyderabad, India, December 2018, pp. 183 – 186.

[3] A. K. Nayak, P. K. Subudhi, S. B. Panda, R. K. Nanda: Dual-Band Circular Polarized Printed Antenna for WiMAX and LTE Applications, Proceedings of the IEEE International Symposium on Smart Electronic Systems (iSES) (Formerly iNiS), Rourkela, India, December 2019, pp. 340 – 343.

[4] H. Kimouche, D. Abed, B. Atrouz, R. Aksas: Bandwidth Enhancement of Rectangular Monopole Antenna Using Modified Semi-Elliptical Ground Plane and Slots, Microwave and Optical Technology Letters, Vol. 52, No. 1, January 2010, pp. 54 – 58.

[5] A. K. Nayak, R. Pachpole, A. Patnaik: Compact Symmetric Quarter Mode Substrate Integrated Waveguide (QMSIW) Antenna, Proceedings of the IEEE Indian Conference on Antennas and Propagation (InCAP), Hyderabad, India, December 2018, pp. 1 – 4.

[6] M. John, M. J. Ammann: Optimization of Impedance Bandwidth for the Printed Rectangular Monopole Antenna, Microwave and Optical Technology Letters, Vol. 47, No. 2, October 2005, pp. 153 – 154.

[7] G. Krishnaveni, B. Manimegalai, B. Saravanya: A Hexagonal Monopole Textile Antenna for UWB Applications, Proceedings of the International Conference on Innovations in Information, Embedded and Communication Systems (ICIIECS), Coimbatore, India, March 2015, pp. 1 – 6.

[8] N. Dhar, M. A. Rahman, M. A. Hossain, A. T. Mobashsher: Bandwidth-Enhanced Metamaterial Integrated Antenna for Wireless Applications, Proceedings of the 5th International Conference on Advances in Electrical Engineering (ICAEE), Dhaka, Bangladesh, September 2019, pp. 117 – 122.

[9] C. A. Balanis: Antenna Theory: Analysis and Design, 2nd Edition, John Wiley & Son, Inc., New York, 1997.

[10] Y. Wang, T. Huang, D. Ma, P. Shen, J. Hu, W. Wu: Ultra-Wideband (UWB) Monopole Antenna with Dual Notched Bands by Combining Electromagnetic-Bandgap (EBG) and Slot Structures, Proceedings of the IEEE MTT-S International Microwave Biomedical Conference (IMBioC), Nanjing, China, May 2019, pp. 1 – 3.

[11] B. Roy, S. K. Chowdhury, A. K. Bhattacharjee: Symmetrical Hexagonal Monopole Antenna with Bandwidth Enhancement Under UWB Operations, Wireless Personal Communications, Vol. 108, May 2019, pp. 853 – 863.

[12] S. Ullah, C. Ruan, M. S. Sadiq, T. U. Haq, W. He: High Efficient and Ultra Wide Band Monopole Antenna for Microwave Imaging and Communication Applications, Sensors, Vol. 20, No. 1, December 2019, p. 115.

[13] S. Park, K.- Y. Jung: Novel Compact UWB Planar Monopole Antenna Using a Ribbon-Shaped Slot, IEEE Access, Vol. 10, June 2022, pp. 61951 – 61959.

[14] L. Sang, J. Xu, Z. Liu, Y. Mei, W. Wang, Z. Shen: Low-RCS UWB Planar Monopole Array Antenna Based on the Optimized Design of the Conductor Layers, IEEE Transactions on Antennas and Propagation, Vol. 71, No. 4, April 2023, pp. 3683 – 3688.

[15] N. V. Shahmirzadi, V. Tyagi, J. Nguyen, R. Kazemivala, N. K. Nikolova, C.- H. Chen: Planar Array of UWB Active Slot Antennas for Microwave Imaging of the Breast, IEEE Transactions on Antennas and Propagation, Vol. 71, No. 4, April 2023, pp. 2946 – 2957.

[16] Y. Zhu, S. Zhang, S. Chen: Vehicle Recognition Based on Carrier-Free UWB Radars Using Contrastive Multi-View Learning, IEEE Microwave and Wireless Technology Letters, Vol. 33, No. 3, March 2023, pp. 343 – 346.

[17] S. Roy, R. Mahin, I. Mahbub: A Comparative Analysis of UWB Phased Arrays with Combining Network for Wireless-Power-Transfer Applications, IEEE Transactions on Antennas and Propagation, Vol. 71, No. 4, April 2023, pp. 3204 – 3215.

[18] G. Pachaiyappan, P. Ramanujam: Design of Low Profile Co-axial Fed High Gain Stacked Patch Antenna for Wi-Fi/WLAN/Wi-Max Applications, Frequenz, Vol. 75, No. 1 – 2, 2021, pp. 27-34.

[19] P. Sambathkumar, K. Ramanujam, P. Ramanujam: Design of 6×2 Linear Feed Antenna Array with Suppressed SLL by Employing CCSRR for Ka-Band and 5G mm-Wave Applications, Applied Physics A, Vol. 129, March 2023, p. 287.

[20] P. Ramanujam, V. Prasad, K. Arunachalam: Design of Reflector Based Dipole Antenna for Sub-6GHz 5G Applications, Proceedings of the IEEE Microwaves, Antennas, and Propagation Conference (MAPCON), Bangalore, India, December 2022, pp. 1661 – 1665.

[21] P. Ramanujam, P. G. Ramesh Venkatesan, M. Ponnusamy, T. K. Sethuramalingam: Design of Miniaturized Dual-Band Filtering Antenna with Improved Selectivity Utilizing Square Complementary Split Ring Resonator for 5G MM-Wave Automobile Applications, International Journal of RF Microwave Computer-Aided Engineering, Vol. 32, No. 11, November 2022, p. e23378.

[22] Z.- M. Du, S.- W. Wong, R.- S. Chen, Y. Li, L.- P. Feng, K.- W. Tam: Wide Bandwidth Ratio of 10-to-1 CPW-Fed Whip Antenna with Improved Radiation Patterns, IEEE Transactions on Antennas and Propagation, Vol. 71, No. 3, March 2023, pp. 2796-2801.

[23] C. M. Dikmen, S. Çimen, G. Çakır: Planar Octagonal-Shaped UWB Antenna with Reduced Radar Cross Section, IEEE Transactions on Antennas and Propagation, Vol. 62, No. 6, June 2014, pp. 2946 – 2953.

P. Zhang, J. Li: Compact UWB and Low-RCS Vivaldi Antenna Using Ultrathin Microwave-Absorbing Materials, IEEE Antennas and Wireless Propagation Letters, Vol. 16, April 2017, pp. 1965 – 1968.